

Extracting Hypernuclear Properties from the $(e, e'K^+)$ Cross Section

Omar Benhar*

INFN and Department of Physics, "Sapienza" University, I-00185 Rome, Italy

(Dated: September 8, 2022)

Experimental studies of hypernuclear dynamics, besides being essential for the understanding of strong interactions in the strange sector, have important astrophysical implications. The observation of neutron stars with masses exceeding two solar masses poses a serious challenge to the models of hyperon dynamics in dense nuclear matter, many of which predict a maximum mass incompatible with the data. In this article, it is argued that valuable new insight may be gained extending the experimental studies of kaon electro production from nuclei to include the $^{208}\text{Pb}(e, e'K^+)^{208}_{\Lambda}\text{Tl}$ process. The connection with proton knockout reactions and the availability of accurate $^{208}\text{Pb}(e, e'p)^{207}\text{Tl}$ data can be exploited to achieve a largely model-independent analysis of the measured cross section. A framework for the description of kaon electro production based on the formalism of nuclear many-body theory is outlined.

I. INTRODUCTION

Experimental studies of the $(e, e'K^+)$ reaction on nuclei have long been recognised as a valuable source of information on hypernuclear spectroscopy. The extensive program of measurements performed and approved at Jefferson Lab [1, 2] —encompassing a variety of nuclear targets ranging from ^6Li to ^{40}Ca and ^{48}Ca —has the potential to shed new light on the dynamics of strong interactions in the strange sector, addressing outstanding issues such as the isospin-dependence of hyperon-nucleon (YN) interactions and the role of three-body forces involving nucleons and hyperons. In addition, because the appearance of hyperons is expected to become energetically favoured in dense nuclear matter, these measurements have important implications for neutron star physics.

The recent observation of two-solar-mass neutron stars [3, 4] —the existence of which is ruled out by many models predicting the presence of hyperons in the neutron star core [5]—suggests that the present understanding of nuclear interactions involving hyperons is far from being complete. In the literature, the issue of reconciling the calculated properties of hyperon matter and massive stars is referred to as *hyperon puzzle* [6].

Owing to the severe difficulties involved in the determination of the potential describing YN interactions from scattering data, the study of hypernuclear spectroscopy has long been regarded as a very effective alternative approach to obtain much needed complementary information.

In this context, the $(e, e'K^+)$ process offers clear advantages. The high resolution achievable by γ -ray spectroscopy can only be exploited to study energy levels below nucleon emission threshold, while (K^-, π^-) and (π^+, K^+) reactions mainly provide information on non-spin-flip interactions. Moreover, compared to hadron induced reactions, kaon electro production allows for a bet-

ter energy resolution, which in turn results in a more accurate identification of the hyperon binding energies [1]. However, the results of several decades of study of the $(e, e'p)$ reaction [7] show that to achieve this goal the analysis of the measured cross sections must be based on a theoretical model taking into account the full complexity of electron-nucleus interactions. Addressing this issue will be critical for the extension of the Jefferson Lab program to the case of a heavy target with large neutron excess, such as ^{208}Pb , best suited to study hyperon dynamics in an environment providing the best available proxy of the neutron star interior.

This article is meant to be a first step towards the development of a comprehensive framework for the description of the $(e, e'K^+)$ cross section within the formalism of nuclear many-body theory, which has been extensively and successfully employed to study the proton knockout reaction [7]. In fact, the clear connection between $(e, e'p)$ and $(e, e'K^+)$ processes, that naturally emerges in the context of the proposed analysis, shows that the missing energy spectra measured in $(e, e'p)$ experiments provide the baseline needed for a largely model-independent determination of the hyperon binding energies.

The text is structured as follows. In Sect. II the description of kaon electro-production from nuclei in the kinematical regime in which factorisation of the nuclear cross section is expected to be applicable is reviewed, and the relation to the proton knockout process is highlighted. The issues associated with the treatment of the elementary electron-proton vertex and the calculation of the nuclear amplitudes comprising the structure of the $^{208}\text{Pb}(e, e'K^+)^{208}_{\Lambda}\text{Tl}$ cross section are discussed in Sect. III. Finally, the summary and an outlook to future work can be found in Sect. IV.

II. THE $A(e, e'K^+)_{\Lambda}A$ CROSS SECTION

Let us consider the kaon electro-production process

$$e(k) + A(p_A) \rightarrow e'(k') + K^+(p_K) + {}_{\Lambda}A(p_R) , \quad (1)$$

* omar.benhar@roma1.infn.it

in which an electron scatters off a nucleus of mass number A , and the hadronic final state

$$|F\rangle = |K^+ \Lambda A\rangle, \quad (2)$$

comprises a K^+ meson and the recoiling hypernucleus, resulting from the replacement of a proton with a Λ in the target nucleus. The incoming and scattered electrons have four-momenta $k \equiv (E, \mathbf{k})$ and $k' \equiv (E', \mathbf{k}')$, respectively, while the corresponding quantities associated with the kaon and the recoiling hypernucleus are denoted $p_K \equiv (E_K, \mathbf{p}_K)$ and $p_R \equiv (E_R, \mathbf{p}_R)$. Finally, in the lab reference frame—in which the lepton kinematical variables are measured— $p_A \equiv (M_A, 0)$.

The differential cross section of reaction (1) can be written in the form

$$d\sigma_A \propto L_{\mu\nu} W^{\mu\nu} \delta^{(4)}(p_0 + q - p_F), \quad (3)$$

with $\lambda, \mu = 1, 2, 3$, where $q = k - k'$ and $p_F = p_K + p_R$ are the four-momentum transfer and the total four-momentum carried by the hadronic final state, respectively. The tensor $L_{\mu\nu}$, fully specified by the electron kinematical variables, can be written in the form [8]

$$L = \begin{pmatrix} \eta_+ & 0 & -\sqrt{\epsilon_L \eta_+} \\ 0 & \eta_- & 0 \\ -\sqrt{\epsilon_L \eta_+} & 0 & \epsilon_L \end{pmatrix}, \quad (4)$$

with $\eta_{\pm} = (1 \pm \epsilon)/2$ and

$$\epsilon = \left(1 + 2 \frac{|\mathbf{q}|^2}{Q^2} \tan^2 \frac{\theta_e}{2} \right)^{-1}, \quad (5)$$

where θ_e is the electron scattering angle, $q \equiv (\omega, \mathbf{q})$, $Q^2 = -q^2$, and $\epsilon_L = \epsilon Q^2 / \omega^2$.

All the information on hadronic, nuclear and hypernuclear dynamics is contained in the nuclear response tensor, defined as

$$W^{\mu\nu} = \langle 0 | J_A^{\mu\dagger}(q) | F \rangle \langle F | J_A^\nu(q) | 0 \rangle, \quad (6)$$

where $|0\rangle$ denotes the target ground state and the final state $|F\rangle$ is given by Eq.(2).

Equation (6) shows that the theoretical calculation of the cross section requires a consistent description of the nuclear and hypernuclear wave functions, as well as of the nuclear current operator appearing in the transition matrix element, J_A^μ . This problem, which in general involves non trivial difficulties, greatly simplifies in the kinematical region in which the impulse approximation can be exploited.

A. Impulse Approximation and Factorisation

Figure 1 provides a diagrammatic representation of the $(e, e' K^+)$ process based on the factorisation *ansatz*. This scheme is expected to be applicable in the impulse approximation regime, corresponding to momentum transfer such that the wavelength of the virtual photon, $\lambda \sim 1/|\mathbf{q}|$, is short compared to the average distance between nucleons in the target nucleus, $d_{NN} \sim 1.5$ fm.

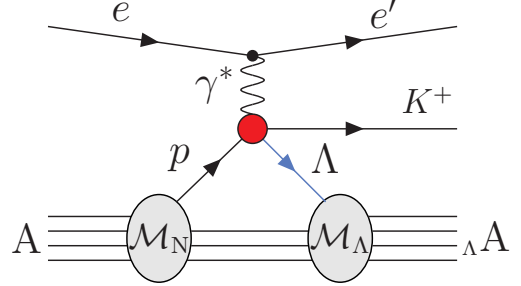


FIG. 1. Schematic representation of the scattering amplitude associated with the process of Eq.(1) in the impulse approximation regime.

Under these conditions, which can be easily met at Jefferson Lab, hereafter JLab, the beam particle primarily interacts with individual protons, the remaining $A - 1$ nucleons acting as spectators. As a consequence, the nuclear current operator reduces to the sum of one-body operators describing the electron-proton interaction

$$J_A^\mu(q) = \sum_{i=1}^A j_i^\mu(q), \quad (7)$$

and the hadronic final state takes the product form

$$|F\rangle = |K^+\rangle \otimes |{}_\Lambda A\rangle, \quad (8)$$

with the outgoing K^+ being described by a plane wave, or by a distorted wave obtained from a kaon-nucleus optical potential [1].

From the above equations, it follows that the nuclear transition amplitude

$$\mathcal{M}^\mu = \langle K^+ {}_\Lambda A | J_A^\mu(q) | 0 \rangle, \quad (9)$$

can be written in factorised form through insertion of the completeness relations

$$\int \frac{d^3 p}{(2\pi)^3} |\mathbf{p}\rangle \langle \mathbf{p}| = \int \frac{d^3 p_\Lambda}{(2\pi)^3} |\mathbf{p}_\Lambda\rangle \langle \mathbf{p}_\Lambda| = \mathbb{1}, \quad (10)$$

where the integrations over the proton and Λ momenta also include a sum over the spins, and

$$\sum_n |(A-1)_n\rangle \langle (A-1)_n| = \mathbb{1}, \quad (11)$$

the sum being extended to all eigenstates of the $(A-1)$ -nucleon spectator system.

The resulting expression turns out to be

$$\mathcal{M}^\mu = \langle K^+ {}_\Lambda A | J_A^\mu | 0 \rangle = \sum_{i=1}^A \sum_n \int \frac{d^3 p}{(2\pi)^3} \frac{d^3 p_\Lambda}{(2\pi)^3} \mathcal{M}_{\Lambda A \rightarrow (A-1)_n + \Lambda}^* \langle \mathbf{p}_K \mathbf{k}_\Lambda | j_i^\mu | \mathbf{p} \rangle \mathcal{M}_{A \rightarrow (A-1)_n + p} , \quad (12)$$

where the current matrix element describes the elementary electromagnetic process $\gamma^* + p \rightarrow K^+ + \Lambda$.

The nuclear and hypernuclear amplitudes in the right-hand side of Eq.(12), labelled \mathcal{M}_N and \mathcal{M}_Λ in Fig. 1, are given by

$$\mathcal{M}_{A \rightarrow (A-1)_n + p} = \{ \langle \mathbf{p} | \otimes \langle (A-1)_n | \} | 0 \rangle , \quad (13)$$

and

$$\mathcal{M}_{\Lambda A \rightarrow (A-1)_n + \Lambda} = \{ \langle \mathbf{p}_\Lambda | \otimes \langle (A-1)_n | \} | {}_\Lambda A \rangle . \quad (14)$$

In the above equations, the states $| (A-1)_n \rangle$ and $| {}_\Lambda A \rangle$ describe the $(A-1)$ -nucleon spectator system, appearing as an intermediate state, and the final-state Λ -hypernucleus, respectively.

The amplitudes of Eq.(13) determine the Green's function describing the propagation of a proton in the target nucleus, $G(\mathbf{k}, E)$, and the associated spectral function, defined as

$$P(\mathbf{k}, E) = -\frac{1}{\pi} \text{Im } G(\mathbf{k}, E) \quad (15)$$

$$= \sum_n |\mathcal{M}_{A \rightarrow (A-1)_n + p}|^2 \delta(E + M_A - m - E_n) ,$$

where m is the nucleon mass and E_n denotes the energy of the $(A-1)$ -nucleon system in the state n . The spectral function describes the *joint* probability to remove a nucleon of momentum \mathbf{k} from the nuclear ground state leaving the residual system with excitation energy $E > 0$.

Within the mean-field approximation underlying the nuclear shell model, Eq.(15) reduces to the simple form

$$P(\mathbf{k}, E) = \sum_{\alpha \in \{F\}} |\varphi(\mathbf{k})|^2 \delta(E - |\epsilon_\alpha|) , \quad (16)$$

where $\alpha \equiv \{nj\ell\}$ is the set of quantum numbers specifying the single-nucleon orbits. The sum is extended to all states belonging to the Fermi sea, the momentum-space wave functions and energies of which are denoted $\varphi_\alpha(\mathbf{k})$ and ϵ_α , respectively, with $\epsilon_\alpha < 0$.

Equation (16) shows that within the independent particle model the spectral function reduces to a collection of δ -function peaks, corresponding to the energy spectrum of the single-nucleon states. Dynamical effects beyond the mean field shift the position of the peaks, that also acquire a finite width. In addition, the occurrence of virtual scattering processes leading to the excitation of nucleon pairs to states above the Fermi surface leads to the appearance of a sizeable continuum contribution, accounting for $\sim 20\%$ of the total strength. As a consequence, the normalisation of a shell model state φ_α ,

referred to as spectroscopic factor, is reduced from unity to a value $Z_\alpha < 1$.

The nuclear spectral functions have been extensively studied measuring the cross section of the $(e, e'p)$ reaction, in which the scattered electron and the knocked out nucleon are detected in coincidence. The results of these experiments, carried out using a variety of nuclear targets, have unambiguously identified the states predicted by the shell model, highlighting at the same time the limitations of the mean-field approximation and the effects of nucleon-nucleon correlations [7, 9].

In analogy with Eqs. (13) and (15), the amplitudes of Eq.(14) comprise the spectral function

$$P_\Lambda(\mathbf{k}_\Lambda, E_\Lambda) = \sum_n |\mathcal{M}_{\Lambda A \rightarrow (A-1)_n + \Lambda}|^2 \quad (17)$$

$$\times \delta(E_\Lambda + M_{\Lambda A} - M_\Lambda - E_n) ,$$

describing the joint probability to remove a Λ from the hypernucleus ${}_\Lambda A$ leaving the residual system with energy E_Λ . Here M_Λ and $M_{\Lambda A}$ denote the mass of the Λ and the hypernucleus, respectively.

The observed $(e, e'K^+)$ cross section, plotted as a function of the missing energy

$$E_{\text{miss}}^\Lambda = \omega - E_{K^+} . \quad (18)$$

exhibits a collection of peaks, providing the sought-after information on the energy spectrum of the Λ in the final state hypernucleus¹.

Note that both the electron energy loss, ω , and the energy of the outgoing kaon, E_{K^+} , are *measured* kinematical quantities.

B. Kinematics

The expression of E_{miss}^Λ , Eq.(18) can be conveniently rewritten considering that the δ -function of Eq.(3) implies the condition

$$\omega + M_A = E_{K^+} + E_{\Lambda A} . \quad (19)$$

Combining the above relation with the requirement of conservation of energy at the nuclear and hypernuclear vertices, dictating that

$$M_A = E_p + E_n , \quad E_\Lambda + E_n = E_{\Lambda A} , \quad (20)$$

¹ In principle, the right-hand side of Eq.(18) should also include a term accounting for the kinetic energy of the recoiling hypernucleus. However, for heavy targets this contribution turns out to be negligibly small, and will be omitted.

we find

$$\omega + E_p = E_{K^+} + E_\Lambda . \quad (21)$$

Finally, substitution into Eq.(18) yields

$$E_{\text{miss}}^\Lambda = E_\Lambda - E_p . \quad (22)$$

The above equation, while providing a relation between the *measured* missing energy and the binding energy of the Λ in the final state hypernucleus, defined as $B_\Lambda = -E_\Lambda$, does not allow for a model independent identification of E_Λ . The position of a peak observed in the missing energy spectrum turns out to be determined by the difference between the energies needed to remove a Λ from the final state hypernucleus, E_Λ , or a proton from the target nucleus, E_p , leaving the residual $(A-1)$ -nucleon system in the same bound state, specified by the quantum numbers collectively denoted n .

The proton removal energies, however, can be independently obtained from the missing energy *measured* in proton knockout experiments, in which the scattered electron and the ejected proton are detected in coincidence, defined as

$$E_{\text{miss}}^p = \omega - E_{p'} = -E_p . \quad (23)$$

where $E_{p'}$ is the energy of the outgoing proton. Note that, consistently with Eq.(18), in the right-hand side of the above equation the kinetic energy of the recoiling nucleus has been omitted.

From Eqs. (22) and (23) it follows that the Λ binding energy can be determined in a fully model independent fashion from

$$B_\Lambda = -E_\Lambda = -(E_{\text{miss}}^\Lambda - E_{\text{miss}}^p) , \quad (24)$$

combining the information provided by the missing energy spectra measured in $(e, e'K^+)$ and $(e, e'p)$ experiments.

III. THE $^{208}\text{Pb}(e, e'K^+)^{208}_\Lambda\text{Tl}$ CROSS SECTION

In view of astrophysical applications, it will be of outmost importance to extend the ongoing experimental studies of kaon electro-production, to include heavy nuclear targets with large neutron excess, such as ^{208}Pb , that provide the best available proxy for neutron star matter. In this section, I will briefly discuss the main elements needed to carry out the calculation of the $^{208}\text{Pb}(e, e'K^+)^{208}_\Lambda\text{Tl}$ cross section within the factorisation scheme illustrated in Section II A.

A. The $e + p \rightarrow e' + K^+ + \Lambda$ process

The description of the elementary $e + p \rightarrow e' + K^+ + \Lambda$ process involving an isolated proton at rest has been obtained from the isobar model [10, 11], in which the hadron

current is derived from an effective Lagrangian comprising baryon and meson fields. Different implementations of this model are characterised by the intermediate states appearing in processes featuring the excitation of resonances [12–14]. The resulting expressions—involving a set of free parameters determined through a fit to the available experimental data—have been employed to obtain nuclear cross sections within the approach based on the nuclear shell model and the frozen-nucleon approximation [1, 12]

In principle, the calculation of the nuclear cross section within the scheme outlined in Sect. II A should be performed taking into account that the elementary process involves a bound, moving nucleon, with four-momentum $p \equiv (E_p, \mathbf{p})$ and energy

$$E_p = m - E , \quad (25)$$

as prescribed by Eq. (15). However, the generalisation of phenomenological approaches constrained by free proton data, such as the isobar model, to off-shell kinematics entails non trivial difficulties.

A simple procedure to overcome this problem is based on the observation that in the scattering process on a bound nucleon, a fraction $\delta\omega$ of the energy transfer goes to the spectator system. The amount of energy given to the struck proton, the expression of which naturally emerges from the impulse approximation formalism, turns out to be [15]

$$\begin{aligned} \tilde{\omega} &= \omega - \delta\omega \\ &= \omega + m - E - \sqrt{m^2 + \mathbf{p}^2} . \end{aligned} \quad (26)$$

Note that from the above equations it follows that

$$E_p + \omega = \sqrt{m^2 + \mathbf{p}^2} + \tilde{\omega} , \quad (27)$$

implying in turn

$$(p + q)^2 = (\tilde{p} + \tilde{\omega})^2 = W^2 , \quad (28)$$

where $\tilde{q} \equiv (\tilde{\omega}, \mathbf{q})$ and $\tilde{p} \equiv (\sqrt{m^2 + \mathbf{p}^2}, \mathbf{p})$.

The above equations show that the replacement $q \rightarrow \tilde{q}$ allows to establish a correspondence between scattering on a off-shell moving proton, leading to the appearance of a final state of invariant mass W , and the corresponding process involving a proton in free space.

It has to be mentioned that, although quite reasonable on physics grounds, the use of \tilde{q} in the hadron current leads to a violation of current conservation. This problem is inherent in the impulse approximation scheme, which does not allow to simultaneously conserve energy and current in correlated systems. A very popular and effective workaround for this issue, widely employed in the analysis of $(e, e'p)$ data, has been first proposed by de Forest in the 1980s [16].

In view of the fact that the extension of the work of Refs.[13, 14] to the case of a moving proton does not involve severe conceptual difficulties, the consistent application of the formalism developed for proton knock-out to

processes the case of kaon electro production appears to be feasible. In this context, it should also be pointed out that the factorisation scheme discussed in Sect. II allows for a fully relativistic treatment of the electron-proton vertex, which is definitely required in the kinematical region accessible at JLab [15].

B. Nuclear and Hypernuclear Dynamics

Vauable information needed to obtain Λ removal energies from the $^{208}\text{Pb}(e, e' K^+) ^{208}_{\Lambda}\text{Tl}$ cross section, using the procedure described in Sect. II B, has been gained by a high-resolution study of the $^{208}\text{Pb}(e, e' p) ^{207}\text{Tl}$ carried out at NIKHEF-K in the late 1980s and 1990s [17–20]. The available missing energy spectra—measured with a resolution of better than 100 KeV and extending up to ~ 30 MeV—provide both position and width of the peaks corresponding to the bound states of the recoiling ^{207}Tl nucleus.

It is very important to realise that a meaningful interpretation of NIKHEF-K data requires the use of a theoretical framework taking into account effects of nuclear dynamics beyond the mean-field approximation. This issue is illustrated in Figs. 2 and 3.

Figure 2 displays the difference between the energies corresponding to the peaks in the measured missing energy spectrum, $\langle E_{\alpha} \rangle$, and the predictions of the mean-field model reported in Ref. [21], E_{HF}^{α} . It is apparent that the value of the quantity

$$\Delta_{\alpha} = |E_{\text{HF}}^{\alpha} - \langle E_{\alpha} \rangle|, \quad (29)$$

where the index $\alpha \equiv \{nj\ell\}$ specifies the state of the recoiling system, is sizeable, and turns out to be as large as ~ 3 MeV for deeply bound states.

Figure 3 provides a comparison between the spectroscopic factors extracted from NIKHEF-K data and the results of the analysis of Ref. [22]. The solid line, exhibiting a remarkable agreement with the experiment, has been obtained combining nuclear matter results, corresponding to the dashed line, and a phenomenological correction accounting for finite size and shell effects. The energy dependence of the spectroscopic factors of nuclear matter at equilibrium density has been derived from a calculation of the pole contribution to the spectral function of Eq. (15), carried out using Correlated Basis Function (CBF) perturbation theory and a microscopic nuclear Hamiltonian including two- and three-nucleon potentials [23].

The results of Fig. 3 show that the spectroscopic factors of the deeply bound proton states of ^{208}Pb are largely unaffected by surface and shell effect, and can be accurately estimated using results of nuclear matter calculations. Finite size effects, mainly driven by long-range nuclear dynamics, are more significant in the vicinity of the Fermi surface, where they account for up to $\sim 35\%$ of the deviation from the mean-field prediction, represented by the solid horizontal line.

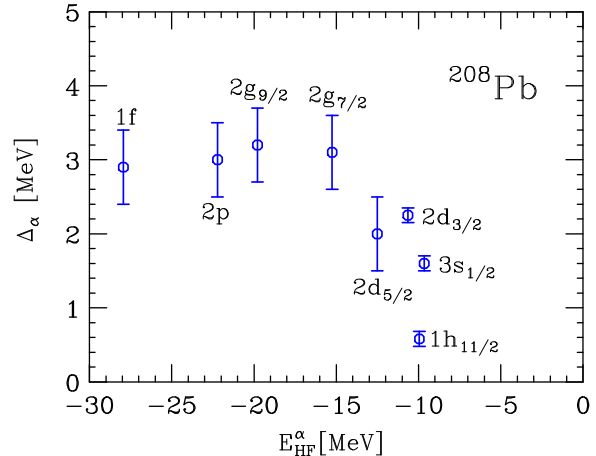


FIG. 2. Difference between the energies corresponding to the peaks in the missing energy spectrum of the $^{208}\text{Pb}(e, e' p) ^{207}\text{Tl}$ reaction reported in Ref. [17] and the theoretical predictions of Ref. [21], obtained within the mean-field approximation. The horizontal axis shows the mean-field energies, and the states are labeled according to the standard spectroscopic notation

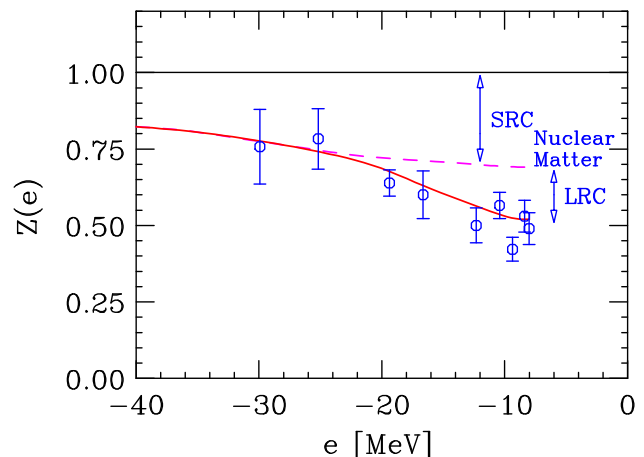


FIG. 3. Spectroscopic factors of the shell model states of ^{208}Pb , obtained from the analysis of the $^{208}\text{Pb}(e, e' K^+) ^{208}_{\Lambda}\text{Tl}$ cross section measured at NIKHEF-K [17]. The solid and dashed lines represent the results of theoretical calculations of the spectroscopic factors of ^{208}Pb and nuclear matter, respectively [22]. For comparison, the horizontal line shows the prediction of the independent particle model. The deviations arising from short- and long-range correlations are highlighted and labelled SRC and LRC, respectively.

In addition to the nucleon spectral function, the analysis of the $^{208}\text{Pb}(e, e' K^+) ^{208}_{\Lambda}\text{Tl}$ cross section requires a consistent description of the Λ spectral function, defined by Eq. (17). Following the pioneering nuclear matter study of Ref. [24], microscopic calculations of $P_{\Lambda}(\mathbf{k}_{\Lambda}, E_{\Lambda})$ in a variety of hypernuclei—ranging from

${}^5_\Lambda\text{He}$ to ${}^{208}_\Lambda\text{Pb}$ —have been recently carried out by the author of Ref. [25]. In this work, the self-energy of the Λ has been obtained from G -matrix perturbation theory in the Brueckner-Hartree-Fock approximation, using the Jülich [26, 27] and Nijmegen [28–30] models of the YN potential.

In view of the fact that the generalisation of the approach of Ref. [25] to treat ${}^{207}\text{Tl}$ using Hamiltonians including YNN potentials does not appear to involve severe difficulties, a fully consistent description of the ${}^{208}\text{Pb}(e, e'K^+){}^{208}_\Lambda\text{Tl}$ process within the factorisation scheme cross section appears to be achievable.

IV. SUMMARY AND OUTLOOK

The results discussed in this article indicate that valuable information on hypernuclear dynamics can be obtained from a largely model independent analysis of the measured ${}^{208}\text{Pb}(e, e'K^+){}^{208}_\Lambda\text{Tl}$ cross section, and that the development of a consistent theoretical framework, allowing to exploit the new data to constrain YN and YNN potential models, can be attained within the well established approach based on nuclear many-body theory and the Green's function formalism.

More recent computational approaches, mostly based on the Monte Carlo method [31], have been very successful in obtaining ground-state expectation values of Hamiltonians involving nucleons and hyperons, see, e.g.

Ref. [6]. However, the present development of these techniques does not allow the calculation of $(e, e'p)$ or $(e, e'K^+)$ cross sections in the kinematical regime in which the underlying non-relativistic approximation is expected to fail. On the other hand, the approach based on factorisation has proved very effective for the interpretation of the available $(e, e'p)$ data.

Owing to the extended region of constant density and the large neutron excess, ${}^{208}\text{Pb}$ is the best available proxy for neutron star matter, and the study of the reaction discussed in this article has obvious astrophysical implications.

The solution of the “hyperon puzzle” is likely to require a great deal of theoretical and experimental work for many years to come. In this context, the extension of the JLab kaon electro production program to ${}^{208}\text{Pb}$ will allow to collect new data useful to understand the effects of three-body forces in a regime in which—based in the present understanding of the non-strange sector—they are expected to be large.

ACKNOWLEDGMENTS

This work was supported by the Italian National Institute for Nuclear Research (INFN) under grant TEON-GRV. The author is deeply indebted to Petr Bydžovský, Franco Garibaldi and Isaac Vidaña for many illuminating discussions on issues related to the subject of this article.

-
- [1] F. Garibaldi *et al* (Jefferson Lab Hall A Collaboration), Phys. Rev. C **99**, 054309 (2019).
 - [2] S. Nakamura, AIP Conference Proceedings **2130**, 020012 (2019).
 - [3] P. Demorest, T. Pennucci, S. Ransom, M. Roberts, and J. Hessels, Nature **467**, 1081 (2010).
 - [4] J. Antoniadis *et al.*, Science **340**, 6131 (2013).
 - [5] I. Vidaña, D. Logoteta, C. Providência, A. Polls, and I. Bombaci, EPL **94**, 11002 (2011).
 - [6] D. Lonardoni, A. Lovato, S. Gandolfi, and F. Pederiva, Phys. Rev. Lett. **114**, 092301 (2015).
 - [7] O. Benhar, Nucl. Phys. News **26**, 15 (2016).
 - [8] E. Amaldi, S. Fubini, and G. Furlan, *Pion Electroproduction* (Springer, Berlin, 1979).
 - [9] S. Frullani and J. Mougey, Adv. Nucl. Phys. **26**, 15 (2016).
 - [10] J. Adam, Jr., J. Mareš, O. Richter, M. Sotona, and S. Frullani, Czech. J. Phys. **42**, 1167 (1992).
 - [11] J.C. David, C. Fayard, G.H. Lamot, and B. Saghai, Phys. Rev. C **53**, 2613 (1996).
 - [12] M. Sotona and S. Frullani, Prog. Theor. Phys. Suppl. **117**, 151 (1994).
 - [13] D. Skoupil and P. Bydžovský, Phys. Rev. C **93**, 025204 (2016).
 - [14] D. Skoupil and P. Bydžovský, Phys. Rev. C **97**, 025202 (2018).
 - [15] O. Benhar, D. Day, and I. Sick, Rev. Mod. Phys. **80**, 189 (2008).
 - [16] T. de Forest, Jr., Nucl. Phys. A **392**, 232 (1983).
 - [17] E.N.M. Quint, *Limitations of the Mean-Field Description for Nuclei in the Pb-Region, Observed with the $(e, e'p)$ Reaction*, Ph.D. thesis, University of Amsterdam (1988).
 - [18] E.N.M. Quint *et al*, Phys. Rev. Lett. **57**, 186 (1986).
 - [19] I. Bobeldijk *et al*, Phys. Rev. Lett. **73**, 2684 (1994).
 - [20] I. Bobeldijk *et al*, Phys. Lett. B **353**, 32 (1995).
 - [21] J.W. Negele and D. Vautherin, Phys. Rev. C **5**, 1472 (1972).
 - [22] O. Benhar, A. Fabrocini, and S. Fantoni, Phys. Rev. C **41**, R24 (1990).
 - [23] O. Benhar, A. Fabrocini, and S. Fantoni, Nucl. Phys. A **505**, 267 (1989).
 - [24] N.J. Robertson and W.H. Dickhoff, Phys. Rev. C **70**, 044301 (2004).
 - [25] I. Vidaña, Nucl. Phys. A **958**, 48 (2017).
 - [26] B. Holzenkamp, K. Holinde, and J. Speth, Nucl. Phys. A **500**, 485 (1989).
 - [27] J. Heidenbauer and U.G. Meissner, Phys. Rev. C **72**, 044005 (2005).
 - [28] P.M.M. Maesen, T.A. Rijken, and J.J. de Swart, Phys. Rev. C **40**, 2226 (1989).
 - [29] T.A. Rijken, V.J.G. Stocks, and Y. Yamamoto, Phys. Rev. C **59**, 21 (1999).
 - [30] V.J.G. Stocks and T.A. Rijken, Phys. Rev. C **59**, 3009 (1999).
 - [31] J. Carlson, S. Gandolfi, F. Pederiva, S. C. Pieper, R. Schiavilla, K. E. Schmidt, and R. B. Wiringa, Rev. Mod.

Phys. **87**, 1067 (2015).